Wideband Spectrum Adaptation Without Coordination

Wei Wang, *Member, IEEE,* Yingjie Chen, Zeyu Wang, *Student Member, IEEE,*
Jin Zhang, *Member, IEEE,* Kaishun Wu, *Member, IEEE,* and Qian Zhang, *Fellow, IEEE*

Abstract—Fixed channelization configuration in today's wireless devices fall inefficient in the presence of growing data traffic and heterogeneous devices. In this regard, a number of fairly recent studies have provided spectrum adaptation capabilities for current wireless devices, however, they are limited to inband adaptation or incur substantial coordination overhead. The target of this paper is to fill the gaps in spectrum adaptation by overcoming these limitations. We propose SEER, a frame-level wideband spectrum adaptation solution which consists of two major components: i) a specially-constructed preamble that can be detected by receivers with arbitrary RF bands, and ii) a spectrum detection algorithm that identifies the desired transmission band in the context of multiple asynchronous senders by exploiting the preamble's temporal and spectral properties. SEER can be realized on commodity radios, and can be easily integrated into devices running different PHY/MAC protocols. We have prototyped SEER on the GNURadio/USRP platform to demonstrate its feasibility. Furthermore, using 1.6GHz channel measurements and trace-driven simulations, we have evaluated the merits of SEER over state-of-the-art approaches.

Index Terms—Spectrum adaptation, channelization, sparse recovery

1 INTRODUCTION

Most of today's wireless devices operate on a set of channels whose bandwidths and central frequencies are preset. This fixed channelization setting worked well in past years, while recently it has become inefficient to support the sky-rocketing growth in traffic demands and the emerging heterogeneous wireless devices. On the one hand, the growing data demands from a new generation wireless devices, such as smartphones, tablets, and wearable devices, are driving current and near future wireless systems towards their capacity limits [1]. Unfortunately, due to limited spectrum, such tremendous data growth cannot be sustained by merely increasing the spectrum allocation, thereby calling for more efficient spectrum usage. On the other hand, the co-existence of heterogeneous channels (e.g., channels in Wi-Fi, ZigBee, Bluetooth) used by these devices causes cross-channel interference, which results in unnecessary spectrum waste [2]. For example, a Wi-Fi node using 40MHz channel can be frequently starved by transmissions on overlapped 20MHz Wi-Fi channels or narrow band ZigBee channels, leaving a large portion of the 40MHz spectrum unused [3].

To improve the spectrum efficiency, both governments [4], [5] and researchers [6]–[8] have realized that flexible channelization should be advocated to embrace fine-grained dynamic access over wide spectrum bands. In the context of flexible spectrum access, wireless devices adaptively select operating channels based on traffic demands, interference, and channel quality. Frame-level spectrum adaptation empowers wireless devices to dynamically access proper spectrum blocks in order to avoid uncoordinated co-channel and cross-channel interferences, as illustrated in Fig. 1. Measurements [9], [10] on 1.5GHz wide spectrum show that senders using monolithic 20MHz channels can transmit only about 6% of the time, while the transmission opportunity can be substantially increased to over 90% when senders are able to adapt spectrum over 80MHz band. In addition, it has been reported that link throughput can be improved significantly by tracking the strongest channel [11]. As the best channel changes quickly [8], [11], [12], it is desirable to promptly adapt spectrum accordingly.

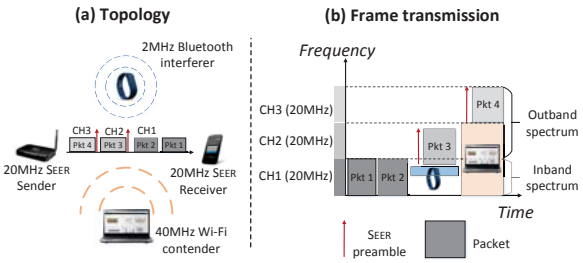

Fig. 1. Illustration of wideband spectrum adaptation. (a) Interference from heterogeneous devices is common in the ISM band. (b) Promptly adapting the transmission band boosts the transmission opportunity, which requires the receiver to detect the transmission band from the aliased spectrum.

Despite growing attempts and extensive efforts, it is still

- *Wei Wang is with the School of Electronic Information and Communications, Huazhong University of Science and Technology and the Guangzhou Fok Ying Tung Research Institute, Hong Kong University of Science and Technology. Correspondence E-mail: gswwang@connect.ust.hk.*
- *Yingjie Chen, Zeyu Wang and Qian Zhang are with the Department of Computer Science and Engineering, Hong Kong University of Science and Technology, Hong Kong.*
- *Jin Zhang is with the Department of Electrical and Electronic Engineering, South University of Science and Technology of China.*
- *Kaishun Wu is with the College of Computer Science and Software Engineering, Shenzhen University.*

challenging to facilitate efficient wideband spectrum adaptation in current wireless devices. State-of-the-art solutions either focus on spectrum adaptation within the transceiver's radio frequency (RF) band [7]–[9] or require central coordination with substantial overhead [6], while the capability of adapting spectrum efficiently over a wideband is still missing. Take Fig. 1 as an example: the 20MHz sender cannot use the adjacent empty spectrum (upper channels in the figure) unless it can adapt to spectrum outside its RF band (outband spectrum). To achieve efficient wideband spectrum adaptation, there are two practical hurdles: i) outband signal detection and ii) spectrum agreement. Most existing approaches detect spectrum using spectrum virtualization techniques [7]–[9], which are limited to signal detection within the receiver's RF band (inband signal detection). What prevents these techniques from outband signal detection is that outband spectrum folds up, resulting in frequency aliasing at the receiver, as shown in Fig. 1(b). Besides, before channel switching, senders and receivers need to agree on the transmission band, which is achieved by central coordination [6] or separate control channels [7]. Unfortunately, these approaches incur substantial overhead and are not prompt enough to respond to frame-level channel variance.

The target of this paper is to fill the gap in wideband spectrum adaptation: we argue that frame-level wideband spectrum adaptation can be realized on commodity radios with lightweight overhead. To achieve this goal, the following requirements should be satisfied. First, there should be no extra coordination for spectrum agreement. Since spectrum adaptation is made at frame-level due to fast fading and traffic dynamics, extra coordination (control messages and channels) should be avoided to minimize overhead. Second, it should be protocol independent. Spectrum adaptation should not rely on specific protocols to maximize the chance of its widespread acceptance. As such, spectrum adaptation can be transplantable to different protocols with only minimal modifications. Finally, it should be easily applied to commodity radios without requiring extra hardware. As such, wideband spectrum adaptation could be smoothly integrated into commercial devices.

To fulfill the aforementioned requirements, this paper introduces SEER (**S**p**E**ctrum adaptation in wid**E**band without coo**R**dination). The core enabling technique of SEER is a wideband-detectable preamble with signatures, which is used to indicate the new transmission band. This preamble is directly prepended to the data frame and is sent and received through the same RF chains used for data transmission. As such, SEER can be applied to different PHY/MAC layers and can be realized without requiring extra hardware. When the sender switches to another channel for transmission, the receiver can identify the new transmission band by analyzing the preamble. Such a preamble eliminates the need for extra control messages, separate control channels, or a central coordinator.

However, it is non-trivial to design such a preamble. A fundamental obstacle is that current radio designs cannot detect signals outside its RF band. The Nyquist-Shannon sampling theorem limits radio's ability of receiving wideband signals: wideband spectrum folds up under aliasing, making signals unrecoverable. To address this predicament, SEER follows on the heels of several recent efforts on sparse recovery [13]–[18], which, however, require certain sparsity in spectrum and thus cannot be directly applied to overcrowded spectrum (e.g., the ISM bands). SEER overcomes this limitation by designing a specially-structured preamble that sustains the sparsity property at a high-power level even when the spectrum is crowded. Another challenge is to use the preamble to notify a SEER receiver of the spectrum occupied by the coming frame in the context of multiple asynchronous senders. Since a SEER receiver needs to switch to the desired spectrum to decode the data frame, spectrum detection should be performed within the preamble time. To this end, SEER exploits the preamble's temporal and spectral properties to identify the spectrum used by the intended frames.

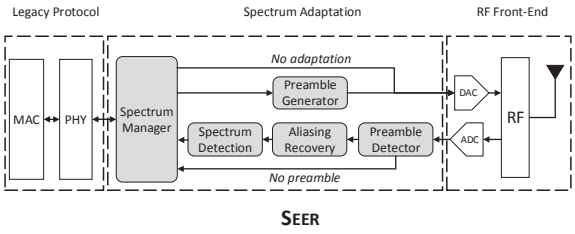

Fig. 2. Architecture of a SEER transceiver.

The main contributions of this paper are summarized as follows. First, we propose a wideband-detectable preamble design on commodity radios. It can be easily integrated to existing devices of different protocols by simply adding spectrum adaptation functions. Second, we implement SEER on the GNURadio/USRP platform to validate the feasibility of our design. To the best of our knowledge, it is the first frame-level wideband spectrum adaptation prototype. Finally, we conduct trace-driven simulations to demonstrate performance the merits of frame-level wideband spectrum adaptation.

The remainder of this paper is structured as follows. We begin in Section 2 with the design overview. Section 3 describes the detailed preamble design to combat frequency aliasing, and Section 4 elaborates on the preamble-based spectrum coding scheme. System implementation and performance evaluation are presented in Section 6. Section 7 describes potential spectrum adaptation applications of our preamble design. Practical issues are discussed in Section 8. Section 9 reviews related work, followed by conclusion in Section 10.

2 Design Overview

The system architecture of SEER is shown in Fig. 2. SEER provides wideband spectrum adaptation capability to wireless devices by adding a decoupled baseband processing layer, referred to as the spectrum adaptation layer, between the legacy physical/media access layer (PHY/MAC) and the RF front-end. The PHY/MAC in a SEER transceiver exposes an interface to the spectrum adaptation layer to allow streams of complex digital baseband samples flowing between the layers. The spectrum adaptation layer adds or removes extra preambles to those baseband samples for spectrum detection

while tuning the RF band through the RF front-end. By decoupling spectrum tuning and detection from packet decoding and scheduling, the legacy PHY/MAC works independently and the spectrum adaptation functionality can be integrated to wireless devices without modifying the radio.

To realize the above abstraction, SEER employs several key components in the spectrum adaptation layer, as depicted in Fig. 2. In the transmitter mode, the preamble generator prepends a specially-constructed preamble to the data frame to convey spectrum information when the transmission band changes. In the receiver mode, SEER devices first detect the specially-designed preamble using the preamble detector, and then identify the new transmission band by two steps: aliasing recovery and spectrum detection. The spectrum manager executes a protocol that decides the spectrum band for packet sending and receiving. Thanks to recent advances in fast channel sensing (e.g., fast wideband sensing [14], [19], probing-free channel tracking [11]) and lightweight feedback (e.g., limited feedback [20], side channels [21]–[23]), the best channel can be obtained with low cost. The spectrum manager is built atop these techniques to acquire channel quality information. In the transmitter mode, the spectrum manager determines the transmission band based on channel quality information, and notifies the preamble generator and the RF front-end if the transmission band changes. In the receiver mode, when the change in the transmission band is detected by the spectrum detector, the spectrum manager tunes the RF band to the detected spectrum for packet receiving.

SEER still conforms the legacy PHY/MAC for packet transmission and channel access. For example, a Wi-Fi based SEER device still needs to contend new channels according to the IEEE 802.11 protocol: after a sender switches to a new transmission band, it still performs CSMA (carrier sense multiple access) protocol as a legacy Wi-Fi node.

The core and challenging part of SEER is to design a preamble that exchanges spectrum information between transceivers. In particular, the preamble must satisfy the following two requirements.

First, the preamble should be detectable and recoverable by a SEER receiver with an arbitrary RF band located in a wide overcrowded spectrum. To support wideband spectrum adaptation without coordination, the preamble must be able to deliver the spectrum information even if the corresponding receiver's RF band is different from the transmission band used for the preamble and the following data frames. Normally, a receiver can only receive and decode inband signals, or sparse signals outside its RF band using sparse recovery techniques. However, the spectrum open to wireless networks is usually overcrowded (e.g., the ISM band), making the outband signals unrecoverable by directly using existing techniques. To overcome this limitation, in Section 3, we design a specially-structured preamble to be recoverable by the receiver whose RF band is different from the sender's.

Second, a SEER receiver can identify the transmission band of its intended frames in the presence of multiple SEER senders. Since preambles are detectable in a wide band, a SEER receiver may detect multiple preambles in the context of multiple SEER senders. The SEER receiver should be able to screen irrelevant preambles and identify the intended transmission band. To support this feature, in Section 4, we elaborate on our design of preamble-based spectrum detection.

3 WIDEBAND-DETECTABLE PREAMBLE DESIGN

The first step towards realizing SEER is to design a wideband-detectable preamble. A fundamental challenge to achieve this goal is frequency aliasing. Modern wireless transceivers are fundamentally gated by the Nyquist rate: the sample rate of a receiver must be at least twice the signal bandwidth. Otherwise, the sample rate is insufficient to capture the changes in the signal, thereby causing frequency aliasing, that is, the signal spectrum folds up and becomes unrecoverable. Sparse recovery techniques [13]–[18] can be leveraged to handle frequency aliasing, while the sparsity condition cannot be satisfied in the commonly-used spectrum which is overcrowded.

To overcome the above hurdle, this section presents the design of a specially-structured preamble to create sparsity in overcrowded spectrum.

3.1 Sparse Recovery

Before presenting the design of the preamble, we first show how frequency aliasing is handled using the latest sparse fast fourier transform (FFT) technique [13], [14] in the case of sparse spectrum.

Aliasing occurs when a receiver captures a spectrum band wider than its own RF band. In particular, when the receiver uses a low-speed analog-to-digital converter (ADC) to sub-sample wideband signals, the wideband signals fold up into the RF band. Formally, denote the width of the RF band as F, the bandwidth of the signal as $W = N \cdot F$ ($N > 1, N \in \mathbb{Z}$). Then, the relationship between the signal's frequency representation $\mathbf{s}$ and the sub-sampled version $\mathbf{s}'$ is given by

$$s'_i = \sum_{n=0}^{N-1} s_{i+nF}, \tag{1}$$

where i is the index for a discrete frequency point in the signal's frequency representation. When a wideband signal is sparse in the frequency domain, i.e., $s_i = 0$ for most frequency points. Then, for a non-zero frequency point s'_i, it is highly-likely to contain only one frequency point $s_{i+kF}, j \in \{0, ..., N-1\}$. In this case, the real frequency position $f = i + kF$ can be derived by shifting s'_i in the time domain, which causes phase rotation in the frequency domain. After shifting the input signal by τ samples, the phase rotation $\Delta\theta$ of s'_i can be used to compute the real frequency position f by:

$$f = \Delta\theta F/(2\pi\tau). \tag{2}$$

A combination of different delays can be used to resolve collisions. For two different signals s_i and $s_{i'}$ that collide at the same sub-sampled frequency position, we can shift the sub-sampled signals twice to obtain the following equation

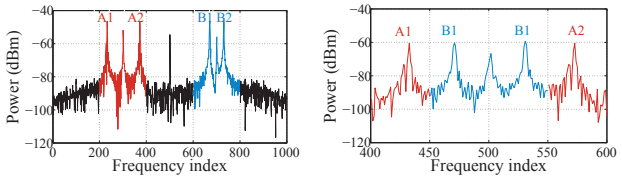

(a) Two concurrent δ-preambles A (red) and B (blue) in 25MHz band.

(b) Received δ-preambles at receivers with 5MHz bandwidth.

Fig. 3. δ-preambles in the frequency domain. Results are taken from a measurement conducted using USRP testbeds. Each δ-preamble consists of two subband signals, which fold up in a 5MHz band at the receiver.

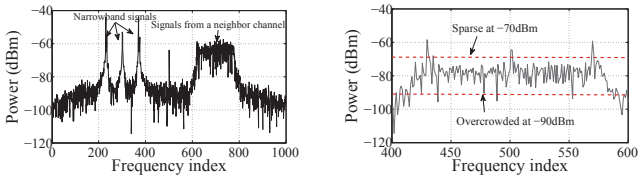

(a) Transmitted 25MHz signals.

(b) Received signals at receivers with 5MHz bandwidth.

Fig. 4. Frequency aliasing. Frequency samples are taken from a measurement conducted using USRP testbeds. High-power narrowband signals create new sparsity in crowded spectrum.

set:

$$\begin{cases} c^0 & = s_i + s_{i'} \\ c^{\tau_1} & = s_i e^{j2\pi f \tau_1/F} + s_{i'} e^{j2\pi f' \tau_1/F} \\ c^{\tau_2} & = s_i e^{j2\pi f \tau_2/F} + s_{i'} e^{j2\pi f' \tau_2/F} \end{cases} \quad (3)$$

where $c^0, c^{\tau_1}, c^{\tau_2}$ are collided signals at the receiver, and f, f' are frequency points of $s_i, s_{i'}$, respectively. Since there are limited number of possible frequency pairs (f, f'), this equation set is solvable.

However, the above technique works well only for sparse spectrum (or differentially sparse spectrum). Unfortunately, the commonly-used spectrum for wireless networks, e.g., the ISM band, is normally overcrowded. In an overcrowded spectrum, most of the frequency points are non-zero, and thus a sub-sampled frequency point normally consists of many different frequency points, making it unlikely for the receiver to recover the real frequency positions. Note that though several fairly recent advances [14], [24] have provided solutions for non-sparse spectrum recovery, they are only applicable to limited scenarios like differentially-sparse spectrum [14] or constellation-sparse signals [24].

3.2 Creating Sparsity in Overcrowded Spectrum

To overcome the aforementioned limitation of sparse recovery, we introduce a preamble structure consisting of multiple narrowband signals to create sparsity in an overcrowded spectrum. Our insight is that even in overcrowded spectrum, high-power signals are still sparse, which is consistent with the results reported in [10]. Then, if we can transmit the preamble using high power, the preamble can be considered as a sparse signal at high-power level. Nevertheless, as the transmission power is limited for a certain device, we cannot simply increase the transmission power to generate high-power preambles. While prior studies [12], [22] have made an observation that a sender using narrower channel can transmit higher magnitude signals. Based on this observation, we design *δ-preamble*[1] which consists of multiple narrowband "pulses" in the frequency domain, as depicted in Fig. 3.

We divide a channel into M equal-width subbands. For example, a 20MHz channel can be divided into 20 subbands of 1MHz bandwidth. Let p_m denote the power of the mth subband. Then, we have $\sum_{m=1}^{M} p_m \leq P$, where P is the total transmission power of the receiver. Then, if we allocate equal power to M' subbands and leave other subbands unused, the power of a used subband is P/M'. Thus, the power of a subband is inversely proportional to the total bandwidth used for transmission. Based on this observation, we can generate multiple high-power subband signals using existing radios without requiring extra transmission hardware or signal processing logic.

The higher magnitude of subband signals creates new sparsity in the frequency domain. As illustrated in Fig. 4, signals from neighboring channels fold up into the receiver's band, resulting in a crowded band full of non-zero frequency points (signals above -90dBm). If we raise the bar to -70dBm, the spectrum is sparse: only three high-power subband signals are above the bar. Then, we can leverage the sparse recovery technique described in Section 3.1 to recover the frequency position of each subband signal in δ-preamble. Since the original frequency position of the δ-preamble can be obtained at the receiver, we can encode the transmission band information and the sender's signature into the δ-preamble using frequency patterns and temporal correlations. Details are elaborated in Section 4.

To recover the frequency of δ-preamble, a practical issue is spectral leakage when generating subband pulses. Since the low pass filter (LPF) is not perfect in practice, generating a high-power subband signal normally attaches several sidelobes to nearby spectrum, which can be misleading when trying to find the right frequency points of pulses. This issue is especially severe when the signal to interference ratio (SIR) is low, in which case the aliasing signals consisting of interference signals and sidelobes are frequently higher than the central peaks of the subband signals. To filter out the peaks generated by sidelobes, we set a threshold (1MHz in our implementation) on the peak searching process to bound the minimal separation between two adjacent pulses, since two adjacent peaks in a δ-preamble are at least one subband's bandwidth away from each other. Note that pulses from different δ-preambles can be differentiated using the temporal correlation properties described in Section 4. Furthermore, we also leverage the redundancy in pulse positions to assist the frequency recovery, as elaborated in Section 4.1.

3.3 Generating δ-Preamble

The δ-preamble can be easily implemented using existing radios without extra hardware. Our goal is to generate multiple

1. Named after the Dirac delta function.

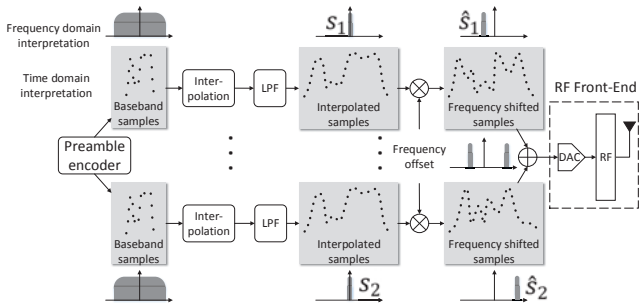

Fig. 5. Preamble generator.

concurrent subband signals using fixed RF front-end hardware. In the transmitter mode, the RF front-end first converts complex digital baseband samples to analog signals spanning the entire bandwidth through a digital-to-analog converter (DAC), and then upconverts the baseband signals to RF signals centered at the sender's carrier frequency. As illustrated in Fig. 5, to generate δ-preamble using the RF front-end, we take the following two steps:

1. Generating pulses. Suppose that the spectrum manager has decided to use which M' subbands out of a total of M subbands to place pulses. According to [25], interpolation in digital samples results in decreased bandwidth. Based on this technique, we interpolate digital samples of each signal by adding $M-1$ duplicated samples, which decreases the bandwidth of the baseband signal to the ratio of $1/M$. As the interpolation process creates aliasing signals, an LPF is added to remove the undesired aliasing signals.

2. Placing pulses. Step 1 creates subband pulses at the central frequency. To generate the δ-preamble, we need to place pulses at corresponding subbands. Let $\mathbf{s} = \sum_{i=0}^{n} s[i]$ be a pulse signal generated in Step 1, and f be the baseband frequency of the desired subband. To place $\mathbf{s}$ in the desired subband, we can simply multiply a frequency offset factor to each sample to derive a frequency shifted signal $\hat{\mathbf{s}} = \sum_{i=0}^{n} s[i]e^{j2\pi if}$. Finally, all pulses are added together before feeding them into DAC, and are transmitted at the sender's carrier frequency. Note that similar techniques have been used to reshape the spectrum for data transmission [8], [26].

3.4 Frequency Recovery of δ-Preamble

When a receiver captures a spectrum band wider than its own RF band, outband signals fold up into its RF band (e.g., in Fig. 3(b), frequencies of four outband pulses A1, A2, B1, B2 moves into the receiver's RF band), thereby requiring the receiver to recover the original frequency of outband signals. As δ-Preamble creates new sparsity in the overcrowded spectrum, we can leverage the latest sparse recovery technique [13], [14] to resolve aliasing and recover the frequency of δ-preamble. However, directly applying this techniques does not perform well due to spectral leakage when generating subband pulses. Since the low pass filter (LPF) is not perfect in practice, generating a high-power subband signal normally attaches several sidelobes to nearby spectrum, which can be misleading when trying to find the right frequency points of pulses. This issue is especially severe when the signal to interference ratio (SIR) is low, in which case the aliasing signals consisting of interference signals and sidelobes are frequently higher than the central peaks of the subband signals. To filter out the peaks generated by sidelobes, we set a threshold (1MHz in our implementation) on the peak searching process to bound the minimal separation between two adjacent peaks, as adjacent pulses in a δ-preamble are at least one subband's bandwidth away from each other. Note that pulses from different δ-preambles can be differentiated using the temporal correlation properties described in Section 4. Furthermore, we also leverage the redundancy in pulse positions to assist the frequency recovery, as elaborated in Section 4.1.

4 Preamble Coding

Given the capability of generating the wideband detectable δ-preamble, the next question is how to leverage the δ-preamble to detect the bandwidth and central frequency of the intended transmission band. We answer this question in this section. We first show how to encode the spectrum information and the sender's signature into the δ-preamble, and then elaborate on the algorithms for preamble detection and transmission band identification.

4.1 Spectrum Information Encoding

Before we start to describe the preamble encoding strategy, we first specify the rules that senders follow to choose the transmission bands.

- **Rule I:** A subband is regarded as a basic unit for spectrum adaptation, and a transmission band is a continuous spectrum band that consists of a set of consecutive subbands.
- **Rule II:** The bandwidth of a transmission band is no wider than the maximal bandwidth supported by the intended receiver's RF front-end.

According to these two rules, a transmission band is represented by a set of consecutive subbands $\{B_l^{sub}, B_{l+1}^{sub}, ..., B_r^{sub}\}$, which can be indicated using a pair of subbands at the band's boundaries (B_l^{sub}, B_r^{sub}). Then, the target of spectrum detection is to identify a pair of subbands (B_l^{sub}, B_r^{sub}) in the wideband spectrum. To this end, we encode the spectrum information by utilizing the frequency structure and temporal correlation simultaneously.

Frequency structure encoding. The δ-preamble consists of multiple subband pulses whose frequencies can be recovered using the technique described in Section 3. SEER utilizes the frequency positions of the pulses to indicate the spectrum band used for data transmission. A naïve method is to place the pulses into predefined subbands. This simple method, however, suffers from high aliasing collision (two pulses collide at the receiver due to aliasing) probability in the presence of multiple SEER senders. Specifically, as the pulse pattern is fixed for all senders, it is likely that all pulses are aliased at the receivers if two senders select the same bandwidth. This case occurs frequently especially for devices with the same ADC sample rate. To address this practical hurdle, we add randomness into the pulse pattern as follows.

In our implementation, a δ-preamble contains four pulses. We place two pulses in the two boundary subbands B_l^{sub} and B_r^{sub}, and the other two pulses in random subbands. In particular, we cut the total transmission band in half, and randomly select one subband from each half band to place a pulse. The total number of subbands is encoded in the signal of the boundary pulses, and the distance between a randomly placed pulse and the boundary subband in the same half band is encoded in the signal of the randomly pulse.

The benefits of this strategy are threefold. First, random placement largely reduces aliasing collision probability when senders select the same bandwidth. Note that though we can recover signals from aliasing collision with high probability, reducing the aliasing collision probability will further improve the recovery rate. In addition, the central frequency and width can be identified even if the frequencies of only two pulses can be recovered. In particular, if a boundary pulse and another pulse is recovered, the boundary pulse can identify the width and the frequency position other pulse can be used identify whether boundary pulse is in the left or the right boundary. The width and position of the boundary pulse can be used to infer the central frequency. Third, if more than two pulses are recovered, the redundancy can set extra constraints in frequency recovery, which in turn improves the accuracy of frequency recovery. To encode the position information in the pulse signals, the encoding strategy must possess the following features.

- **Robust decoding.** Since there are collisions and interference caused by frequency aliasing, the coding scheme must be very robust to combat strong interference. The modulation and coding schemes used for data transmission fails to satisfy this requirement as these schemes normally require high SIR for synchronization, channel estimation, and data decoding.
- **Sender recognition.** In the context of multiple SEER senders, pulses generated by the paired sender must be recognized within the preamble time. Otherwise, the receiver cannot switch to the correct transmission band to decode the intended data frame. One might think of buffing all data samples first and then adopting try-and-error to find the right data frame. However, this approach is inapplicable since aliased high bit-rate data signals are unrecoverable.

To overcome the above challenges, SEER employs temporal correlation encoding strategy to convey the pulse position information and senders' signatures.

Temporal correlation encoding. Motivated by the robust synchronization and sender recognition mechanism adopted in cellular networks, SEER leverages polyphase sequence [27] to encode the pulse position information. Polyphase sequences have long been used in many air interfaces in cellular networks, e.g., the Primary Synchronization Signal (PSS), random access preamble (PRACH), and uplink control channel (PUCCH). In particular, orthogonal sequences are assigned to different base stations (BSs), who multiply their signals by assigned sequences to reduce the cross-correlation of simultaneous transmissions. In practice, the *Walsh-Hadamard codes*

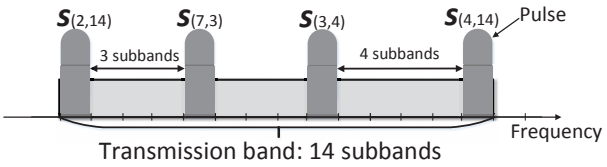

Fig. 6. Encoding spectrum information using δ-preamble.

and the *Zadoff-Chu sequences* (ZC sequences) [28] are used in the Universal Mobile Telecommunications System (UMTS) and the Long Term Evolution (LTE), respectively.

In this paper, we select the ZC sequence, which is defined as:

$$s(u,k)[n] = e^{-j2\pi u \frac{(n-k)(n-k+1)}{2N_z}}, \tag{4}$$

where the sequence index u can be any integer between 0 and N_z that is a relative prime to N_z, N_z the sequence length, $n = 0, 1, ..., N_z - 1$, and k the cyclical-shift parameter. The ZC sequence exhibits the following desirable properties: i) The auto correlation of a prime length ZC sequence with a cyclically shifted version of itself is zero, and ii) The cross-correlation between two prime length ZC sequences is a constant $1/\sqrt{N_z}$, given that the index difference is relative prime to N_z. The strong correlation properties make the ZC sequence ideal for identification: as proposed to the LTE, a unique pair (u, k) can be assigned to a device as its signature.

In our design, we divide the pair (u, k) of ZC sequence into two dimensions: the sequence index u is used to identify the sender, and the cyclic-shift parameter k is used to indicate the pulse position. Recall that a δ-preamble consists of an array of M' pulses that can be expresses as an array of ZC sequence $[s(u_1, k_1), ..., s(u_{M'}, k_{M'})]$. SEER uses the array of sequence indices $u_1, ..., u_{M'}$ as a sender's signature, and the cyclic-shift parameter k_i of a pulse $s(u_i, k_i)$ to indicate the number of subbands between the pulse $s(u_i, k_i)$ and the boundary subband in the same half band. Fig. 6 shows an example of how to encode a δ-preamble consisting of four pulses, where the sender's signature is $[2, 7, 3, 4]$. After successfully detecting the spectrum, the SEER receiver switches channel to the new band to receive incoming frames. Since channel switching incurs extra delay (e.g., 25 μs [29]), which requires a time gap between the δ-preamble and the frame to allow the receiver to switch to the new band before frame transmission. We repeat the δ-preamble multiple times to fill this gap for channel reservation.

The preamble encoding procedure is summarized in Algorithm 1. The sender first selects four subbands – two boundary subbands B_l^{sub}, B_r^{sub} and two random subbands B_p^{sub}, B_q^{sub} – to transmit ZC sequences. The ZC sequences $\{s(u_i, k_i) : i = 1, 2, 3, 4\}$ are configured to contain the sender's signature and pulse position information. The index parameters form an array $[u_1, u_2, u_3, u_4]$ to express the sender's signature. The cyclic-shift parameters $\{k_i : i = 1, 2, 3, 4\}$ indicate pulse positions: the total number of subbands $r - l$ is encoded in k_1, k_4 whose corresponding ZC sequences are placed at boundary subbands, while the relative distances between the

B_l^{sub}, B_p^{sub} and B_q^{sub}, B_r^{sub} are encoded in k_2 and k_3, respectively. Consequently, the δ-preamble consists of four ZC sequences placed at the selected subbands.

Algorithm 1: Preamble Encoding

Data: A transmission band represented by a set of consecutive subbands $\{B_l^{sub}, B_{l+1}^{sub}, ..., B_r^{sub}\}$; the sender's signature $[u_1, u_2, u_3, u_4]$
Result: A δ-preamble
1 Select four subbands for pulses: B_l^{sub}, B_r^{sub}, and randomly pick $B_p^{sub}, B_q^{sub} \in \{B_{l+1}^{sub}, ..., B_{r-1}^{sub}\}$;
2 Set pulse position indication parameters: $k_1 = k_4 = r - l; k_2 = p - l; k_3 = r - q$;
3 Generate four ZC sequences: $s(u_1, k_1)$, $s(u_2, k_2)$, $s(u_3, k_3)$, $s(u_4, k_4)$;
4 Place $s(u_1, k_1)$, $s(u_2, k_2)$, $s(u_3, k_3)$, $s(u_4, k_4)$ at $B_{l+1}^{sub}, B_p^{sub}, B_q^{sub}, B_{r-1}^{sub}$, respectively;
5 δ-preamble $\leftarrow$ summation of the four pulses $\{s(u_i, k_i) : i = 1, 2, 3, 4\}$ at baseband;

4.2 Preamble Decoding

Pulse Detection. The relatively high power of pulses make them easy to detect. A SEER device leverages energy detection method that is inherently enabled by the device. For example, an IEEE 802.11 device detects the start of an incoming signal by measuring the energy of the sampled signal $\mathbf{s}$: $P_s = \sum_{k=1}^{L} |s[k]|^2$, where L is the measuring window. The high-power pulses are easy to detect by this method when when there is no frequency aliasing. However, when the receiver's band is filled with aliased signals, P_s can be higher than the threshold even if there is no pulses. In this case, the incoming pulses cannot be detected by comparing P_s with the threshold, thereby causing false negatives. To address this predicament, SEER uses the differential rather than the absolute values of P_s for energy detection. When the incoming signals are detected, the receiver computes the power spectral density by performing FFT to identify the position of pulses using the technique described in Section 3.1.

Decoding. After the pulse detection, a SEER receiver then determines: i) whether the incoming pulse is from the intended sender, and ii) what is the central frequency and bandwidth used for the following data transmission. In particular, SEER in parallel correlates each pulse signal samples with the N_z sequences in a pipeline fashion, which processes the incoming sample sequence sample by sample in real time and derives the correlation results roughly at the same time when all samples are received. After identifying the parameters (u, k) of pulses, the receiver executes sequential search to find a matched signature. If there are T concurrent transmitters, the sequential searching takes $O(M'T)$ time. There are two extra constraints that further narrow down the search space: i) the frequency separation between pulses in a signature must be consistent with cyclic-shift parameters, ii) the cyclic-shift parameters of boundary pulses are zero.

The receiver runs Algorithm 2 to detect the transmission band of the intended sender. The receiver first performs differential energy detection to detect the presence of any δ-preamble (lines 1-2), and identifies the frequency of each pulse $s[u_i, k_i]$ by FFT and sparse recovery and the parameters (u_i, k_i) by correlation (lines 3-5). Then, the receiver searches all pulses to find the sequence of pulses whose $\{u_i\}$ matches the sender's signature (line 6). Finally, the receiver determines the transmission band based on $\{k_i\}$ and the true frequency of each pulse (lines 7-8).

Algorithm 2: Preamble Decoding

1 **while** *Measure the energy of sampled signals* $\mathbf{s}$ *at time* t*:* $P_s[t] = \sum_{k=1}^{L} |s[k]|^2$ **do**
2 **if** $P_s[t+1] - P_s[t] > \eta_e$ **then**
3 Compute $FFT(\mathbf{s})$;
4 Identify frequency of each pulse $s[u_i, k_i]$ in $\mathbf{s}$ by performing sparse recovery;
5 Identify the parameters $(u_i, k_i), \forall i$ by correlation;
6 Match the sender's signature with $\{u_i : \forall i\}$;
7 Determine the boundary subbands B_l^{sub}, B_r^{sub} based on $\{k_i : \forall i\}$ and pulse frequencies;
8 Transmission band $\leftarrow \{B_l^{sub}, B_r^{sub}\}$
9 **end**
10 **end**

5 IMPLEMENTATION

SEER can be realized in existing OFDM PHY using commodity radios. Note that we require a wider LPF in RF front-end for sparse recovery [14]. We implement the entire baseband design of SEER directly in the USRP Hardware Drive (UHD). Nodes in our experiments are USRP N210 devices equipped with RFX2450 daughterboards as RF frontend, which operates in the 5.1-5.2GHz range. Each sender is connected to a DELL Optiplex desktop with Intel i3 Dual-core processor and 4 GB memory, while each receiver is connected to a Lenovo ThinkCentre desktop with Intel i7 Quad-core processor and 8 GB memory.

We have empowered the δ-preamble generation and detection, frequency aliasing recovery, and spectrum detection using the GNURadio/USRP platform. Due to large processing delay of USRP hardware and limited power of general purpose processor, the spectrum adaptation strategy cannot be performed in real-time on USRP. Thus, we emulate the spectrum adaptation strategy offline using the signals captured by the off-the-shelf Intel 5300 NICs, as well as the spectrum measurements from [10].

6 EVALUATION

We evaluate SEER in this section. In particular, we evaluate the pulse recovery and spectrum detection performance using USRP testbeds.

6.1 Frequency Recovery Performance

A basic primitive of SEER is to recover the frequency of pulses using the method described in Section 3. In this experiment, we use USRP testbeds to verify the robustness of frequency recovery in different SIR environments and the presence of concurrent senders.

Experimental setup. Due to the limited bandwidth and capacity of USRP, we set a channel as 5MHz instead of

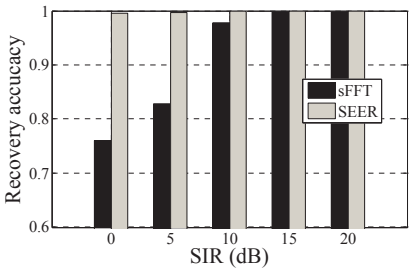

Fig. 7. Frequency recovery accuracy comparison.

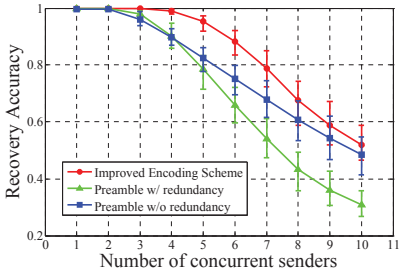

Fig. 8. Frequency recovery accuracy under various number of concurrent senders. SIR = 5dB.

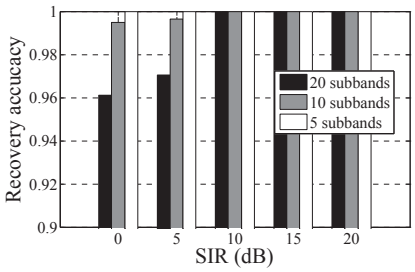

Fig. 9. Frequency recovery accuracy under various number of subbands per channel.

20/40MHz as considered in our design. The transmitted signals are spread in a 25MHz band between 5.1-5.2GHz, and a receiver's bandwidth is set to 5MHz. We use a USRP to send 5MHz frames back-to-back in an adjacent channel to generate aliased interference. The USRP nodes are placed at different locations in a 10m $\times$ 10m office. The experiment is repeated 10,000 times to compute recovery accuracy. We compare the proposed approach (SEER) that is tailored to pulse recovery with a baseline approach (sFFT) that directly applies the state-of-the-art sparse FFT technique [14] without considering sidelobe issues and pulse redundancy.

Comparison with sFFT. Fig. 7 compares the frequency recovery performance of SEER and sFFT in various SIR channels. The results show that SEER achieves almost perfect recovery performance in all cases demonstrated. In 10-20dB SIR range, both approaches achieve over 98% accuracies. When the SIR drops to 0dB, in which case most packet delivery fails, SEER still yields over 99% accuracy, while the recovery accuracy of sFFT drops quickly to 76%. The reason why SEER is more robust than sFFT in low SIR environments is that SEER considers sidelobe issues and leverages redundancy among pulses to assist frequency estimation.

Impact of concurrent senders. In Fig. 8, we vary the number of concurrent SEER senders, who randomly select 5MHz from the total 25MHz band to send δ-preambles. The SIR at the receiver is fixed at 5dB so that we can focus on the impact of concurrent senders. We divide one channel into 20 subbands, and each δ-preamble consists of four subbands. Therefore, the power of δ-preamble in this experiment is $20/4 = 5\times$ of the power for data transmission, which is under the limit of FCC's regulation [30]. We compare our encoding scheme with two baseline schemes: *preamble without redundancy* that places two pulses at boundary subbands, and *preamble with redundancy* as proposed in [31], in which two pulses are used to indicate one boundary subband. The results show that the improved encoding scheme proposed in this paper yields more than 95% accuracy for less than five concurrent senders, and outperforms the other two schemes in all cases demonstrated. The accuracies of all schemes drop significantly when the number of concurrent senders exceed five. This is because the collision probability is high as each sender selects two or four subbands out of 20 subbands in the channel. Note that the chance is rare for more than five senders sending frames simultaneously in one channel. Besides, more concurrent senders can be supported when the number of subbands in one channel is larger (i.e., in a wider channel). Thus, we claim that the frequency recovery function of SEER works well in the presence of multiple senders.

Impact of number of subbands. Fig. 9 shows the recovery accuracy of SEER under different number of subbands in each channel.The number of subbands stands for the frequency estimation granularity. The results show that the it is more robust to divide a channel into less subbands due to the lower granularity requirements. However, reducing the number of subbands involves a adaptation flexibility penalty, as the subband is the basic unit in spectrum adaptation. The figure also shows that the performance of SEER using 10 subbands/channel exhibits only minor degradation with respect to the performance using 5 subbands/channel. We conclude that 10 subbands/channel provides a good compromise between adaptation flexibility and recovery accuracy.

6.2 Spectrum Detection Performance

Experimental setup. We evaluate the spectrum detection performance of SEER using USRP testbeds with the same setup as for frequency recovery evaluation. We use two metrics: *true positive* (TP) rate, i.e., the probability of correctly detecting the intended spectrum, and *false positive* (FP) rate, the probability of falsely recognizing other senders as the intended sender.

Impact of SIR. Fig. 10 shows the spectrum detection accuracy using different sequence lengths N_z. We see that for SIR ≥ 0, the TP rates of two sequences are higher than 97%, while the FP rates are lower than 2.6%, which demonstrates that SEER can detect spectrum with extremely high accuracy in a wide SIR range. Note that the frame delivery rate of Wi-Fi transmissions at SIR $=$ 0dB is less than 10%. Thus, we conclude that SEER yields high accuracy in spectrum detection even in severe interfered channels.

Impact of concurrent senders. Fig. 11 evaluates the spectrum detection performance of SEER in the presence of multiple concurrent senders. A various number of concurrent senders randomly select a channel to transmit δ-preambles, which are aliased at the receiver's RF band. The results show that when the number of concurrent senders is no more than 5, SEER achieves the TP rates higher than 94% and the FP rates lower than 3.7%. When the number of concurrent senders is

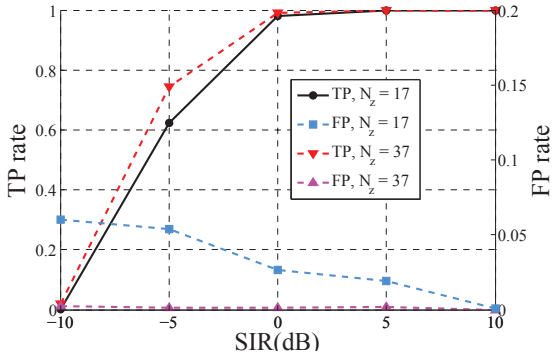

Fig. 10. TP and FP rates under various SIR.

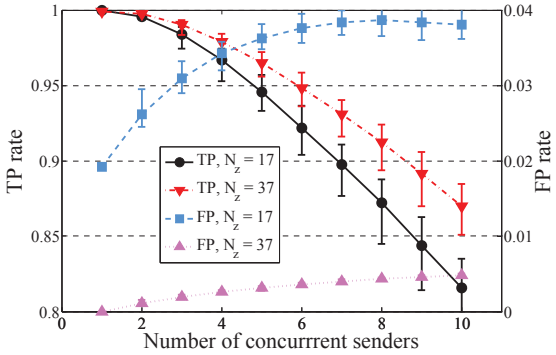

Fig. 11. TP and FP rates under various number of concurrent senders. SIR = 5dB.

increased to 10, the TP rate of SEER with $N_z = 17$ drop to 82%, while the FP rate is still less than 4%. Regarding that the chance of more than 5 concurrent senders is very low (e.g., CSMA-based networks use random backoff mechanism to avoid collision), SEER achieves high accuracy in most cases.

Impact of number of subbands and channel width. Fig. 12 shows the spectrum detection accuracy as a function of the number of subbands per channel. The number of concurrent senders is set to be 5. The detection accuracy goes up with the number of subbands per channel as there are less collision probability. When the number of subbands per channel is larger than 10, SEER with different N_z achieves TP rates over 94% and FP rates below 4%, which shows that dividing a 20/40MHz channel into 2MHz subbands is a feasible setting. Fig. 13 shows that SEER performs better in wider channels, as there are more subbands in one channel.

7 SEER APPLICATIONS IN SPECTRUM ADAPTATION

So far we have elaborated how SEER enables a transmission pair to change channels using δ-preamble. In this section, we discuss the applications of SEER in Wi-Fi spectrum adaptation and dynamic spectrum access.

7.1 Per-Frame Spectrum Adaptation in Wi-Fi

We first present the MAC design of SEER that incorporates the wideband spectrum adaptation capability into the MAC adopted by legacy Wi-Fi.

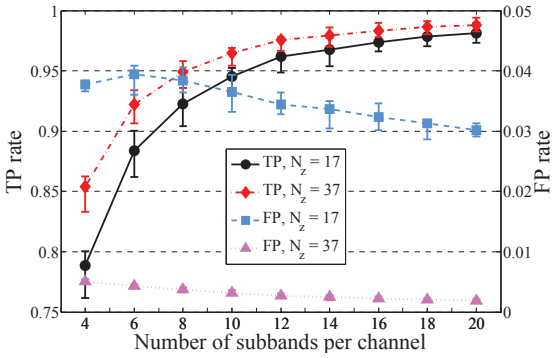

Fig. 12. TP and FP rates under under various number of subbands per channel. The number of concurrent senders is 5. SIR = 5dB.

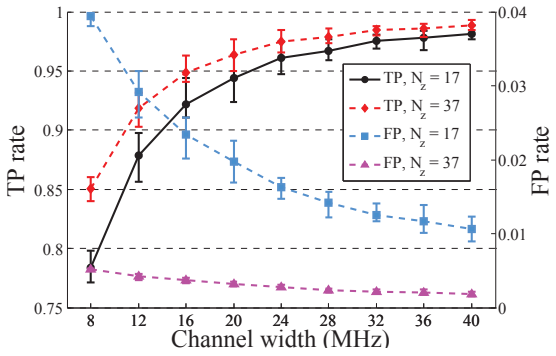

Fig. 13. TP and FP rates under channels with various bandwidths.

The main challenge in the SEER MAC is how to sustain the benefits of spectrum adaptation while incurring minimal overhead. Prior to spectrum adaptation, a sender needs to scan the wideband spectrum to determine the central frequency and channel width for the subsequent packet transmissions. The wideband scanning can be efficiently achieved by adopting existing wideband sensing techniques such as [14], [19], and the best channel can be tracked by a single probing [11]. To avoid unnecessary overhead, SEER employs a spectrum adaptation strategy in MAC to trigger the adaptation process. In the following part of this section, we discuss the SEER MAC in both distributed Wi-Fi networks and centralized enterprise WLANs, respectively.

SEER MAC in distributed Wi-Fi networks. In distributed Wi-Fi networks, transmission pairs are uncoordinated. SEER triggers spectrum adaptation only when the channel availability or quality is unable to support reliable transmission. A SEER sender transmits legacy frames unless i) the current channel is busy, or ii) the quality of current channel is low. We adopt two metrics – *transmission opportunity* and signal-to-noise ratio (SNR) – to estimate the channel conditions. The transmission opportunity is defined to be the ratio of successful transmissions to the total number of transmission attempts. Only when the transmission opportunity or the SNR falls below the predefined threshold, the sender to adapt to a new channel. To be compatible to legacy Wi-Fi nodes, SEER nodes still conform to the legacy DCF MAC (e.g., IEEE

802.11a/g/n/ac) to contend channels. In particular, SEER nodes sense channel, backoff, and transmit as the legacy nodes. When the spectrum adaptation is triggered, SEER nodes sense the wideband spectrum and identify the best channel based on existing techniques [11], [14]. Then, SEER nodes switch to new spectrum, and contend channels according to the legacy DCF MAC.

SEER MAC in centralized enterprise WLANs. Different from the distributed Wi-Fi networks, in centralized enterprise WLANs, all access points (AP) are connected via an Ethernet backhual and are managed by a central controller. Analogous to existing scheduling algorithms [6], [8] in enterprise WLANs, we focus on the downlink traffic. The metrics that trigger spectrum adaptation are the same as used in the distributed Wi-Fi networks, while the central frequencies and channel widths are determined by the central controller. The central controller uses the following greedy spectrum adaptation strategy to assign channels. When a SEER sender suffers from low transmission opportunity or low SNR, it sends a spectrum adaptation request to the central controller via backhual. The central controller re-allocates spectrum to the sender by going through all possible channels. In particular, the central controller goes through all possible channels, and selects the solution that maximizes the overall throughput in the WLAN. There are two choices for each node whose operating channel is the selected new band: i) it stays in the channel and contends the channel with the new comer, or ii) it swaps its operating channel with the new comer's. The central controller computes the overall throughput by measuring the SNR of each channel and mapping the SNR to corresponding data rate according to [32]. Then, the central controller selects the spectrum adaptation solution that maximizes the overall throughput. Note that if none of the adaptation solutions can improve the overall throughput compared to the original channel assignment, the central controller calls off the adaptation.

Signature Distribution. In centralized mode, such as enterprise WLANs, the signatures are assigned by a central controller to avoid signature ambiguity. While in ad hoc mode, each SEER sender randomly pick an array $u_1, ..., u_{M'}$ as its signature. In both modes, a sender's signature is delivered to the corresponding receiver in association. We set N_z to be a prime number, e.g., 17, 31, thereby allowing u to be any integer between 0 and N_z. Thus, there are a total of $(N_z-1)^{M'}$ different arrays that can be used as signatures. The probability of two SEER senders selecting the same signature is $\frac{1}{(N_z-1)^{M'}}$, which is significantly small. In our implementation, the probability is $\frac{1}{(N_z-1)^{M'}} = \frac{1}{(17-1)^4} = 1.5 \times 10^{-5}$.

Due to the strong correlation properties of ZC sequence, collision occurs only when two collided pulses select the same (u, k) pair. This event is highly unlikely to occur because it requires that all of the following four events occur at the same time: i) two SEER senders send δ-preamble simultaneously, ii) two pulses are aliased at the receivers, iii) two pulses pick the same sequence index u, and iv) two pulses have the same distance to the boundary subband (i.e., use the same cyclic-shift parameter k). Therefore, ambiguity and collision of concurrent transmitted δ-preambles occur with only very small probabilities, thereby having minimal impact on the performance of SEER.

Interoperability with Legacy Wi-Fi. Since SEER still conforms to the legacy DCF at MAC layer, SEER nodes can coexist with legacy nodes. Concretely, SEER nodes precisely follow the MAC protocol specified by IEEE 802.11 to contend channel with other legacy nodes – SEER nodes will defer if they sense a transmission of IEEE 802.11 nodes and vice versa. As SEER nodes have more flexibility in spectrum allocation, which offers them more transmission opportunities and may cause unfairness to legacy nodes. A potential solution to alleviate the unfairness issue is to increase the DIFS of SEER nodes when they change their channels, which gives legacy nodes higher priority in competition with the new comers. To further understand this solution, we need to study the impact of tuning DIFS. The expected transmission opportunities can be computed based on DIFS, backoff counter, as well as the number of channels. To ensure fairness, we enforce the expected transmission opportunity of each node to be equal.

7.2 Trace-Driven Evaluation

The primary motivation of SEER is that the spectrum is used more efficiently when nodes can adaptively access spectrum according to channel availability or quality variance. The objective of this section is to show the efficacy of SEER in promptly adapting spectrum according to channel availability and quality variances. Due to the processing delay, USRP cannot support real-time MAC layer protocols. Thus, we turn to trace-driven simulations to evaluate the merits of wideband spectrum adaptation enabled by SEER. We use the spectrum measurements in [10] as channel availability variance, and collect CSI traces using Intel 5300 NICs to log channel quality variance.

Simulation methodology. To study the performance of SEER, we take Wi-Fi as a study case and implement an emulator to model the CSMA/CA MAC as in 802.11. We compare SEER with two baseline approaches: fixed channelization (FIXED) and inband spectrum adaptation (INBAND). FIXED selects the operating channel based on initial measurements and will not change channel during the simulation. INBAND is capable of per-frame inband adaptation as described in [8]. We take into account the spectrum adaptation overhead ($31\mu s$) when simulating SEER. For fair comparison, we adopt the same spectrum adaptation strategy as described earlier for INBAND and SEER. The channel bandwidth, or the RF bandwidth of each node, is set to be 20MHz. INBAND can use noncontinuous fragments in a channel while SEER can use a continuous band over a wide spectrum.

Channel availability trace. We use the extensive spectrum occupancy measurements provided by [10] as channel availability trace. We select the channel measurements that span 1.6GHz wide spectrum centered at 5.25GHz, which indicate the 5GHz ISM band usage pattern. Measurements are collected using Agilent E4440A spectrum analyzer which sweeps over the 1.6GHz spectrum every 1.8s with granularity of 200KHz. Note that the 1.8s interval is sufficient to capture the channel usage pattern [33].

Channel quality trace. We also log the fine-grained channel quality variance using Intel 5300 NICs. We use Intel 5300 NICs to send back-to-back frames and log the CSI and SNR traces at receivers. We vary the sender and receiver's locations to measure 20 different links, whose SNR vary from -3dB to 28dB. Each link transmits 500 frames for every 20MHz channels across an entire 80MHz band using the methodology adopted in [11].

Evaluation of SEER under channel availability variance. Fig. 14 evaluates the performance of SEER using the channel availability trace. We assume that there is a single transmission link with saturated traffic. The sender transmits 1000-Byte frames at 54Mbps. All approaches can use up to a channel bandwidth to transmit frames, while SEER can select a band no wider than a channel width from a wide band, whose bandwidth is referred to as *searching bandwidth*. The searching bandwidth of SEER is set to be the width of five channels in Fig. 14(a) and Fig. 14(b), but varies in Fig. 14(c). The entire 1.6GHz spectrum is divided into continuous 20/40MHz channels.

Fig. 14(a) and Fig. 14(b) compare the throughput in all channels of the entire 1.6GHz spectrum. We set five channels as a group for evaluation, where FIXED and INBAND randomly pick one of the five channels while SEER can adaptively access spectrum no wider than a channel bandwidth within the five channels. The results show that in the entire 1.6GHz spectrum, SEER significantly outperforms INBAND and FIXED. In the range of 4.45-5.45GHz, the spectrum is heavily-used, FIXED and INBAND do not have enough flexibility to avoid pervasive interference, while SEER is still able to find short transmission opportunities.

Fig. 14(c) evaluates the impact of searching bandwidth on SEER's performance. We randomly select a central frequency in the 1.6GHz spectrum and repeat simulations to obtain the average throughput. The figure shows that the average throughput increases with the searching bandwidth, which demonstrates the benefits of wideband spectrum adaptation.

Evaluation of SEER under channel quality variance. In Fig. 15, we evaluate the the performance of SEER using the fine-grained channel quality trace. Similar to [6], [8], we consider an enterprise WLAN setting where a central controller dynamically assigns channel to each link. FIXED adopts static channel assignment that is optimal with regard to the initial channel quality. As optimal channel assignment is NP-hard, we adopt a heuristic algorithm for INBAND and SEER similar to [8]: when a link suffers from SNR lower than a threshold, the central controller swaps this link with another link that gives the largest improvement. INBAND can only swap two links in the same 20MHz channel, while SEER lifts this restriction.

We feed saturated traffic to each link, which is randomly mapped to a link in the collected trace. Data rate for each transmission is selected based on the link's SNR according to the standard SNR-data rate mapping table as listed in [32].

Fig. 15(a) varies the number of links accessing the 80MHz spectrum, which consists of four 20MHz channels. The results show that on average, SEER outperforms FIXED and INBAND by 102% and 37%, respectively. This observation demonstrates that SEER can use spectrum more efficiently by adaptively accessing the spectrum. When the number of links goes larger than 10, the throughput of all approaches decreases due to larger contention overhead. Fig. 15(b) further compares the performance of all approaches under when varying the total bandwidth. The number of links is set to 8. By leveraging the frequency diversity of multiple channels, SEER achieves higher throughput than the other two approaches when there are more than one channel.

Fig. 15(c) shows the impact of the trigger threshold. When the threshold is higher, both approaches have more chances to trigger spectrum adaptation, thereby yielding higher throughput. We also observe that the throughput increases quickly at first, while becoming plateaued when the threshold is larger than 8dB, which reveals that the performance gain of spectrum adaptation mainly comes from poor links with low SNR. This observation shows that we can avoid unnecessary overhead and still achieve most throughput gain by setting a reasonable trigger threshold.

8 DISCUSSION

Some practical issues are discussed in this section.

8.1 Scalability

Supporting concurrent transmissions. Although the δ-preamble is designed to support concurrent transmissions, the number of concurrent preambles is limited to less than ten to achieve reasonable performance. Fortunately, such limitation fits well in Wi-Fi networks. Note that 2.4GHz Wi-Fi band is around 100MHz. Thus, the cases where more than ten concurrent transmissions are very rare. In addition, since Wi-Fi adopts the random backoff mechanism, the chance of concurrent preamble transmissions is very low. Our evaluation results have shown that SEER achieves the TP rates higher than 94% and the FP rates lower than 3.7% when the number of concurrent senders is 5. Therefore, our design is able to support concurrent transmissions in Wi-Fi.

Signature distribution scalability. Another scalability issue is related to signature distribution in dense environments with many active nodes. In a typical dense network case given in the latest IEEE 802.11 scenario [34], the total number of users within contention range is 64. In our current implementation where the length of ZC sequence is set to be 17, the probability of a user's signature colliding with others' is $64/(17-1)^4 = 0.097\%$, which is even much lower than the packet collision probability. Therefore, the signature collision probability in Wi-Fi scenario is negligible.

8.2 Spectrum Adaptation Overhead

The spectrum adaptation latency is mainly caused by the preamble detection and channel switching. The airtime for δ-preamble transmission is proportional to $\frac{N_z}{W_s}$. In our design, we set $N_z = 17$ and $W_s = 2$MHz, which result in $8.5\mu s$ airtime for δ-preamble transmission. Recall that the preamble detection algorithm takes $O(M'T)$ time where T is the number of concurrent SEER senders and M' is

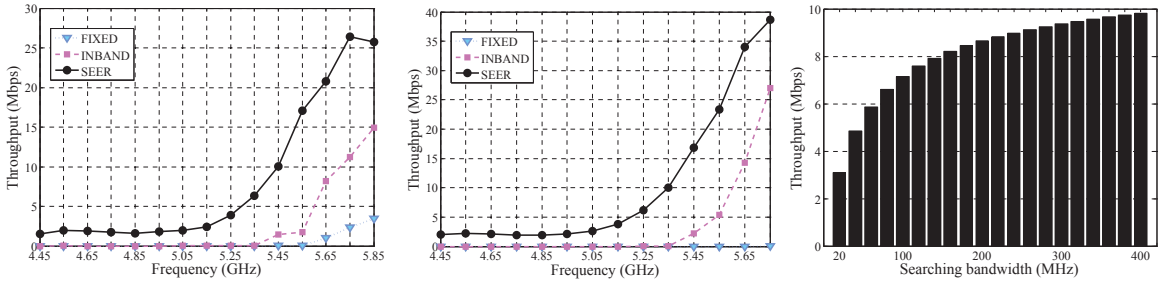

(a) Throughput comparison using 20MHz channel. Searching bandwidth of SEER is 100MHz.

(b) Throughput comparison using 40MHz channel. Searching bandwidth of SEER is 200MHz.

(c) Average throughput of SEER under different searching bandwidth. Channel width is 20MHz.

Fig. 14. Throughput of SEER using the 1.6GHz wide spectrum availability trace.

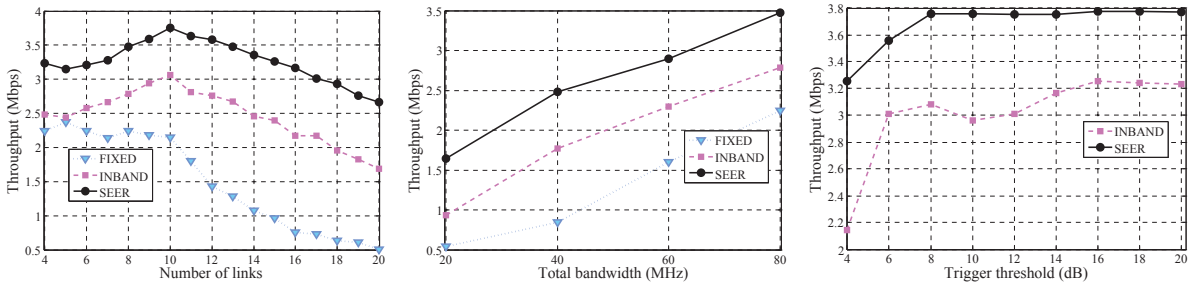

(a) Throughput versus number of links.

(b) Throughput versus total bandwidth.

(c) Throughput versus trigger threshold.

Fig. 15. Throughput comparison using the channel quality trace.

the number of pulses in a δ-preamble. When there are five concurrent SEER senders, the preamble detection algorithm takes merely $0.5\mu s$ with a 40MHz digital signal processor ($M' = 4$ in our implementation). Hence, the latency incurred by the preamble detection is $8.5 + 0.5 = 9\mu s$, which adds $9/(101.5+224+20+62) = 2.2\%$ overhead to a typical IEEE 802.11 packet transmission at 54Mbps.

Channel switching latency is mainly contributed by the lock-in time of the phase-locked loop (PLL) used by the transceiver's chipset. The off-the-shelf 802.11 chipset incurs $25\mu s$ latency for channel switching within 100MHz range [29], while state-of-the-art in solid state electronics has shown that this latency can be less than $22\mu s$ for channel switching within 1.9GHz [35]. These delays could be further reduced in future integrated circuit (IC) designs. Therefore, the overall spectrum adaptation latency is $9+22 = 31\mu s$, which is merely 7.6% of the total time used for a 54Mbps 802.11 packet transmission.

Recall that recent advances have made it feasible to promptly acquire channel availability and quality in a wide spectrum with low overhead. For example, scanning a 0.9GHz spectrum to acquire channel availabilities takes merely $1\mu s$ with 50MHz/s ADCs [14], and reliably estimating the strongest channel from a set of channels only requires measurements collected on a single channel without extra channel probings [11]. Therefore, we conclude that finding and adapting to the best spectrum are fast enough to enable frame-level spectrum adaption.

9 Related Work

Dynamic spectrum access. Dynamic spectrum access allows devices to dynamically change their operating central frequency and spectrum bandwidths. Chandra et al. [12] have shown that it is beneficial for Wi-Fi nodes to adapt channel width according to transceiver's requirements and environmental conditions. Jello [36] extends bandwidth adaptation to non-continuous channel bonding in the case of narrowband interference, but it requires coordination for spectrum agreement. Yun et al. [8] devise an efficient per-frame spectrum adaptation solution for Wi-Fi networks by exploiting 802.11 preamble structure. These studies demonstrate that dynamically changing channel width and central frequency largely improves throughput compared with fixed-channel configurations. However, these solutions are limited to spectrum adaptation within the receiver's RF band, and none of them supports outband spectrum adaptation. There are several recent works [14], [19] on wideband spectrum sensing, which is the basis for wideband spectrum adaptation. SEER is complimentary to wideband spectrum sensing by supporting per-frame outband spectrum detection and spectrum agreement.

Spectrum allocation. Flexible channelization mechanisms have been proposed to adaptively allocate fine-grained spectrum bands on the basis of traffic demands and wireless environments. WhiteFi [37] constructs a Wi-Fi like system which incorporates an adaptive spectrum assignment algorithm in TV band. It detects transmissions of variable channel bandwidth by analyzing ACK time duration, which requires buffering the raw signal of the whole frame. However, WhiteFi requires that that the central frequencies of a transmission pair are aligned. FLUID [6] builds a conflict model for flexible channelization and allocates flexible channels to APs in an enterprise network. A central controller is introduced to assign flexible channels to APs, who notify clients about channel

switch using beacons. Different from FLUID, SEER adapts spectrum without coordination and central controller.

Spectrum virtualization. Spectrum virtualization is proposed in many recent works [7], [9], [26] to change spectrum in baseband without RF modifications. These solutions leverage signal shaping techniques such as sampling rate conversion and frequency shifting to change spectrum with little overhead. Picasso [26] and SVL [7] create an extra spectrum shaping layer for general wireless devices. However, they do not consider spectrum agreement between sender and receiver. RODIN [9] uses an extra FPGA-based spectrum shaper and a new preamble to enable per-frame spectrum adaptation and agreement on commercial devices. However, SEER is fundamentally different from these spectrum virtualization techniques in that spectrum virtualization alters spectrum within RF band, while SEER enables outband spectrum adaptation.

Sparse Recovery. Our outband signal detection design is closely related to sparse FFT [13], [14] and compressive sensing techniques [15]–[18]. The original work on sparse Fourier transform [13] provides fundamental theories to apply sparse FFT to wide band spectrum sensing. BigBand [14] is the first work to utilize sparse FFT to realize GHz-wide realtime spectrum sensing. However, BigBand is based on multiple co-prime ADCs in a receiver, thereby requiring new hardware design at receivers. Similar to sparse FFT, compressive sensing techniques [15]–[18] achieve sub-Nyquist sampling by adding an extra GHz analog mixer before low rate ADC to perform high-speed complex analog matrix multiplications and analog mixing. There are two fundamental differences between SEER and these sparse recovery studies. First, these techniques require customized hardware or multiple co-prime ADCs at receivers, while SEER can be applied on commercial devices without these hardware modifications. Second, these sparse recovery proposals focus on spectrum sensing and are not capable of differentiating the transmitter of a certain spectrum, and thus it cannot be directly applied to outband spectrum adaptation.

10 CONCLUSION

This paper presents SEER, the first system design and prototype for frame-level wideband spectrum adaptation. SEER leverages a specially-constructed preamble and a robust spectrum detection scheme to support coordination-free spectrum adaptation in wide spectrum beyond the receiver's RF band. We have prototyped SEER using the GNURadio/USRP platform, and demonstrate its feasibility and substantial benefits through extensive experiments and simulations. We hope the design of SEER can contribute the wireless community by improving the spectrum efficiency to mitigate overcrowding of unlicensed spectrum usage. In particular, we envision that the prompt spectrum adaptation capability brought by SEER can alleviate the cross interference between heterogeneous devices, improve the spectrum efficiency in crowded WLANs, and enable cognitive radios using today's RF hardware with minimal modifications.

SEER can be realized on commodity radios and integrated into wireless devices running different protocols without special hardware. SEER is a clean solution that is independent and transparent to PHY/MAC protocols. We believe that with these features, SEER can be easily applied to a wide-range of devices.

ACKNOWLEDGMENT

We gratefully acknowledge the use of wireless data from Spectrum Data Archive of the Institute of Networked Systems at RWTH Aachen University. The research was supported in part by grants from China NSFC under Grant 61502114, 61173156, 973 project 2013CB329006, ITS/143/14FP-A, RGC under the contracts CERG MHKUST609/13 and 622613, Shenzhen Science and Technology Foundation KQCX20150324160536457, Guangdong Young Talent Project 2014TQ01X238.

REFERENCES

[1] Qualcomm, "Rising to meet the 1000x mobile data challenge," http://www.qualcomm.com/media/documents/rising-meet-1000x-mobile-data-challenge.
[2] W. Wang, Y. Chen, Q. Zhang, and T. Jiang, "A software-defined wireless networking enabled spectrum management architecture," *IEEE Commun. Mag.*, vol. 54, no. 1, pp. 33–39, 2016.
[3] V. Shrivastava, S. Rayanchu, J. Yoonj, and S. Banerjee, "802.11 n under the microscope," in *Proc. ACM IMC*, 2008.
[4] FCC, "Second memorandum opinion and order (FCC 10-174)," 2010.
[5] PCAST, "Report to the president: Realizing the full potential of government-held spectrum to spur economic growth," 2012.
[6] S. Rayanchu, V. Shrivastava, S. Banerjee, and R. Chandra, "Fluid: improving throughputs in enterprise wireless lans through flexible channelization," in *Proc. ACM MobiCom*, 2011.
[7] K. Tan, H. Shen, J. Zhang, and Y. Zhang, "Enable flexible spectrum access with spectrum virtualization," in *Proc. IEEE DySPAN*, 2012.
[8] S. Yun, D. Kim, and L. Qiu, "Fine-grained spectrum adaptation in wifi networks," in *Proc. ACM MobiCom*, 2013.
[9] E. Chai, J. Lee, S.-J. Lee, R. Etkin, and K. G. Shin, "Building efficient spectrum-agile devices for dummies," in *Proc. ACM MobiCom*, 2012.
[10] M. Wellens and P. Mähönen, "Lessons learned from an extensive spectrum occupancy measurement campaign and a stochastic duty cycle model," *Mobile networks and applications*, vol. 15, no. 3, 2010.
[11] S. Sen, B. Radunovic, J. Lee, and K.-H. Kim, "Cspy: finding the best quality channel without probing," in *Proc. ACM MobiCom*, 2013.
[12] R. Chandra, R. Mahajan, T. Moscibroda, R. Raghavendra, and P. Bahl, "A case for adapting channel width in wireless networks," in *Proc. ACM SIGCOMM*, 2008.
[13] H. Hassanieh, P. Indyk, D. Katabi, and E. Price, "Nearly optimal sparse fourier transform," in *Proc. ACM STOC*, 2012.
[14] H. Hassanieh, L. Shi, O. Abari, E. Hamed, and D. Katabi, "Bigband: Ghz-wide sensing and decoding on commodity radios," in *Proc. IEEE INFOCOM*, 2014.
[15] J. Laska, W. Bradley, T. W. Rondeau, K. E. Nolan, and B. Vigoda, "Compressive sensing for dynamic spectrum access networks: Techniques and tradeoffs," in *Proc. IEEE DySPAN*, 2011.
[16] M. Rashidi, K. Haghighi, A. Panahi, and M. Viberg, "A nlls based sub-nyquist rate spectrum sensing for wideband cognitive radio," in *Proc. IEEE DySPAN*, 2011.
[17] J. Yoo, S. Becker, M. Loh, M. Monge, E. Candes, and A. Emami-Neyestanak, "A 100mhz–2ghz 12.5 x sub-nyquist rate receiver in 90nm cmos," in *Proc. IEEE RFIC*, 2012.
[18] Y.-C. Chen, L. Qiu, Y. Zhang, Z. Hu, and G. Xue, "Robust network compressive sensing," in *Proc. ACM MobiCom*, 2014.
[19] S. Yoon, L. E. Li, S. C. Liew, R. R. Choudhury, I. Rhee, and K. Tan, "Quicksense: Fast and energy-efficient channel sensing for dynamic spectrum access networks," in *Proc. IEEE INFOCOM*, 2013.
[20] D. J. Love, R. W. Heath, V. K. Lau, D. Gesbert, B. D. Rao, and M. Andrews, "An overview of limited feedback in wireless communication systems," *IEEE J. Sel. Areas Commun.*, vol. 26, no. 8, 2008.
[21] J. Zhang, H. Shen, K. Tan, R. Chandra, Y. Zhang, and Q. Zhang, "Frame retransmissions considered harmful: improving spectrum efficiency using micro-acks," in *Proc. ACM MobiCom*, 2012.
[22] A. Cidon, K. Nagaraj, S. Katti, and P. Viswanath, "Flashback: Decoupled lightweight wireless control," in *Proc. ACM SIGCOMM*, 2012.

[23] H. Li, K. Wu, Q. Zhang, and L. M. Ni, "Cuts: Improving channel utilization in both time and spatial domain in wlans," *IEEE Trans. Parallel Distrib. Syst*, vol. 25, no. 6, pp. 1413–1423, 2014.

[24] F. Lu, P. Ling, G. M. Voelker, and A. C. Snoeren, "Enfold: Downclocking ofdm in wifi," in *Proc. ACM MobiCom*, 2014.

[25] A. V. Oppenheim, R. W. Schafer, J. R. Buck *et al.*, *Discrete-time signal processing*. Prentice-hall, 1989.

[26] S. S. Hong, J. Mehlman, and S. Katti, "Picasso: flexible rf and spectrum slicing," in *Proc. ACM SIGCOMM*, 2012.

[27] P. Fan and M. Darnell, *Sequence design for communications applications*. Research Studies Press, 1996.

[28] R. L. Frank, "Polyphase codes with good nonperiodic correlation properties," *IEEE Trans. Inf. Theory*, vol. 9, no. 1, 1963.

[29] Maxim, "MAX2828/MAX2829 world-band transceiver ICs datasheets," http://datasheets.maximintegrated.com/en/ds/MAX2828-MAX2829.pdf.

[30] V. Kone, L. Yang, X. Yang, B. Y. Zhao, and H. Zheng, "Fcc part 15: Radio frequency devices," in *Proc. ACM IMC*, 2010.

[31] W. Wang, Y. Chen, Z. Wang, J. Zhang, K. Wu, and Q. Zhang, "Changing channel without strings: Coordination-free wideband spectrum adaptation," in *Proc. IEEE INFOCOM*, 2015.

[32] H. Rahul, F. Edalat, D. Katabi, and C. G. Sodini, "Frequency-aware rate adaptation and mac protocols," in *Proc. ACM MobiCom*, 2009.

[33] V. Kone, L. Yang, X. Yang, B. Y. Zhao, and H. Zheng, "On the feasibility of effective opportunistic spectrum access," in *Proc. ACM IMC*, 2010.

[34] K. Shin, I. Park, J. Hong, D. Har, and D.-H. Cho, "Per-node throughput enhancement in wi-fi densenets," *IEEE Commun. Mag.*, vol. 53, no. 1, pp. 118–125, 2015.

[35] J. Shin and H. Shin, "A 1.9–3.8 ghz fractional-n pll frequency synthesizer with fast auto-calibration of loop bandwidth and vco frequency," *IEEE J. Solid-State Circuits*, vol. 47, no. 3, 2012.

[36] L. Yang, W. Hou, L. Cao, B. Y. Zhao, and H. Zheng, "Supporting demanding wireless applications with frequency-agile radios," in *Proc. USENIX NSDI*, 2010.

[37] P. Bahl, R. Chandra, T. Moscibroda, R. Murty, and M. Welsh, "White space networking with wi-fi like connectivity," in *Proc. ACM SIGCOMM*, 2009.

Wei Wang (S'10-M'16) is currently a Research Assistant Professor in Fok Ying Tung Graduate School, Hong Kong University of Science and Technology (HKUST). He received his Ph.D. degree in Department of Computer Science and Engineering from HKUST. Before he joined HKUST, he received his bachelor degree in Electronics and Information Engineering from Huazhong University of Science and Technology, Hubei, China, in June 2010. His research interests include privacy preservation and fault management in wireless networks.

Yingjie Chen received his M.Phil. degree of computer science department from Hong Kong University of Science and Technology in 2012. He is currently a reseach assistant in Hong Kong University of Science and Technology. His research interests include PHY and MAC layer design in Wi-Fi network, and mobile computing.

Zeyu Wang received his B.S. degree of computer science from Shanghai Jiao Tong University in 2013. He is currently a Ph.D. candidate in Hong Kong University of Science and Technology. His research interests includes visible light communication, wireless communication and mobile computing.

Qian Zhang (M'00-SM'04-F'12) joined Hong Kong University of Science and Technology in Sept. 2005 where she is Tencent Professor of Engineering and Chair Professor in the Department of Computer Science and Engineering. Before that, she was in Microsoft Research Asia, Beijing, from July 1999, where she was the research manager of the Wireless and Networking Group. She is a Fellow of IEEE for "contribution to the mobility and spectrum management of wireless networks and mobile communications". Dr. Zhang received the B.S., M.S., and Ph.D. degrees from Wuhan University, China, in 1994, 1996, and 1999, respectively, all in computer science.

Kaishun Wu (S'08-M'11) is a distinguished professor in Shenzhen University. He has co-authored 2 books and published over 70 refereed papers in international leading journals and primer conferences. He is the inventor of 6 US and 43 Chinese pending patents (13 are issued). He won the best paper awards in IEEE Globecom 2012, IEEE ICPADS 2012 and IEEE MASS 2014. He received 2014 IEEE ComSoc Asia-Pacic Outstanding Young Researcher Award and selected as 1000 Talent Plan for Young Researchers.

Jin Zhang (S'06-M'09) is currently an assistant professor in Electrical and Electronic Department, South University of Science and Technology of China. She graduated from Department of Electronic Engineering at Tsinghua University in 2004 with a bachelor's degree and in 2006 with a master's degree. She received the Ph.D. degree from Department of Computer Science and Engineering, Hong Kong University of Science and Technology. Her research interests are mainly in next-generation wireless networks, network economics, mobile computing in healthcare, cooperative communication and networks.